Reversible Reactions of Cycloalkane Solvent Holes. 1. Complexation of *cis*- and *trans*-Decalin$^{\bullet+}$ with Alcohols

I. A. Shkrob,* M. C. Sauer, Jr., and A. D. Trifunac

Chemistry Division, Argonne National Laboratory, Argonne, Illinois 60439

Received: November 10, 1999; In Final Form: February 4, 2000

It is shown that solvent holes in *cis*- and *trans*-decalin form complexes with aliphatic alcohols that live 1−100 ns, depending on the solute and the solvent temperature. This complexation has near-zero activation energy and occurs with rate constants of $(1-1.2) \times 10^{11}$ M^{-1} s^{-1} in *trans*-decalin and 3×10^{10} M^{-1} s^{-1} in *cis*-decalin. The metastable complex decays by proton transfer (for alcohols higher than ethanol); in concentrated solutions a diffusion-controlled reaction of the complex with a second alcohol molecule occurs. While the stability of the complex increases with the carbon number of the alcohol, the standard heat of the complexation decreases in the opposite direction ($\Delta H°$ changes from −39 kJ/mol for ethanol to −25 kJ/mol for *tert*-butanol). The decrease in the standard entropy is small ($\Delta S°_{298} > -80$ J mol^{-1} K^{-1}), approaching zero for higher alcohols. We argue that this thermochemistry is due to the polaronic nature of the solvent holes.

1. Introduction

Ionization of saturated hydrocarbon liquids yields quasi-free and solvated electrons and solvent holes (radical cations). Of these two, the holes are more important because their breakup accounts for a large share of C−C and C−H fission products formed after the ionization.[1,2] Studies of the solvent holes are impeded by their short lifetimes and lack of signature absorption bands. For many hydrocarbons, the holes decay either by proton transfer to the solvent or fragmentation; typical lifetimes of the holes are between 1 and 30 ns.[1−4] A few exceptions to this rule are high-mobility solvent holes in four cycloalkanes (cyclohexane, methylcyclohexane, and *cis*- and *trans*-decalins) that live as long as microseconds, depending on the solvent purity.[5−14] Consequently, the chemistry of the solvent holes is best known for these four cycloalkanes; solvent holes in other hydrocarbons are presumed to follow the same reaction pattern. In this series, we focus on a single aspect of this chemistry: "slow" proton transfer from the solvent holes to aliphatic alcohols and benzene. Our study indicates a complex mechanism for this transfer and sheds new light on the nature and reactivity of the solvent holes in general.

In pure liquid *cis*- and *trans*-decalins, the solvent holes live longer than 2 μs.[5,7−11,13] At 25 °C, the mobility, μ_h, of the holes is 5.9 times (*cis*-decalin) or 17.3 times (*trans*-decalin) higher than the combined mobility $\mu_i = \mu_+ + \mu_-$ of molecular ions[5,15] in the solution.[5,9,11] The μ_h/μ_i ratio rapidly decreases with increasing solvent temperature (Table 1). In *trans*-decalin, the migration of the solvent hole is thermoneutral (-3 ± 1 kJ/mol)[5,11] while in *cis*-decalin it is slightly activated (7 ± 2 kJ/mol).[11] These activation energies are much lower than the activation energies for the migration of molecular ions (Table 1).

Not only do the decalin holes migrate rapidly, they also react rapidly.[5,7,8,10,13,14] The fastest known reactions are those of electron transfer from aromatic hydrocarbons and amines.[5,10,13,14] The gas-phase ionization potential (IP_g) of decalins is 9.24−9.26 eV.[16] Aromatic hydrocarbons with $IP_g < 8.82$ eV scavenge the solvent holes with rate constants of 3.5×10^{11} M^{-1} s^{-1} in *trans*-decalin and 5×10^{10} M^{-1} s^{-1} in *cis*-decalin (see below). Proton-transfer reactions of decalin holes are considerably slower than these electron-transfer reactions.[8,10,13] From previous works, some of these reactions appeared to be *very* slow, for no apparent reason: For example, in *trans*-decalin, for several proton-accepting solutes (e.g., 2-propanol and benzene) the scavenging rate constants have been measured as $\approx 5 \times 10^9$ M^{-1} s^{-1},[8,10,13] which is comparable to those for diffusion-controlled reactions of normally diffusing species (at 25 °C).[9]

TABLE 1: Reaction Constants and Migration Parameters for Solvent Holes and Molecular Ions in *cis*- and *trans*-Decalin Liquids

parameter	*trans*-decalin	*cis*-decalin
μ_h [a]	8.7 ± 0.2	1.7 ± 0.1
	9.0[g]	2.0[g]
μ_i [a]	0.52[g]	0.34[g]
	(0.085)[h]	(0.039)[h]
$\nu = \mu_h/\mu_i$ [a,b]	17.3[g]	5.9[g]
E_a (ν)[c]	-16 ± 0.5	-12 ± 1
E_a (μ_h)[c]	-3 ± 1	7 ± 2
	-2.6 ± 1.2[h]	
E_a (μ_i)[c]	13.7 ± 1	21.2 ± 0.7
	13.2 ± 0.4[h]	20.2 ± 0.7[h]
k_{et} [d]	29 ± 0.7	5.05 ± 0.26
E_a (k_{et})[c]	0.94 ± 0.1	6.7 ± 0.4
ϵ[e]	2.15	2.19
$-\partial\epsilon/\partial T$[e]	1.21 ± 0.02	1.17 ± 0.02
ρ, g/cm^3 [f]	0.885	0.912
$-\partial\rho/\partial T$[f]	7.5	7.65
mp, °C[i]	−32	−43
r, nm[j]	0.471	0.482

[a] $\times 10^{-7}$, m^2 V^{-1} s^{-1}; at 25 °C, ref 10. [b] At 25 °C. [c] Activation energy, kJ/mol, ref 11. [d] Scavenging with triphenylene, $\times 10^{10}$ M^{-1} s^{-1} (includes volume expansion; this work). [e] Static dielectric constant and its temperature gradient ($\times 10^{-3}$) at 25 °C, from ref 15. [f] Density and its temperature gradient ($\times 10^{-3}$) at 25 °C; from refs 15 and 35. [g] Reference 5; values in the parentheses are mobilities μ_+ of molecular cations. [h] Reference 15. [i] Melting point, ref 34. [j] Molecular radius estimated from the molar volume b in the van der Waals isotherm, ref 28.

* To whom the correspondence should be addressed.

10.1021/jp993988w CCC: $19.00
Published on Web 03/22/2000

Even more surprisingly, some of these solutes (such as 1-propanol) scavenge *cis*-decalin$^{\bullet+}$ much faster than *trans*-decalin$^{\bullet+}$ (2.6×10^{11} M^{-1} s^{-1} vs 5.3×10^{9} M^{-1} s^{-1}),[10] though the former species is 4.5 times less mobile than the latter (at 25 °C). Warman et al.[8] determined the hole-scavenging constants for several olefins in *trans*-decalin; all of these solutes had higher IP_gs than the solvent which precluded the occurrence of the electron transfer. No correlation was found between the solute proton affinity and these scavenging rate constants. We also did not find such a correlation in our studies.[13]

Such oddities suggest that proton-transfer reactions of cycloalkane holes have complex mechanisms. Warman et al. suggested that scavenging of decalin holes by proton acceptors proceeds through the formation of a short-lived complex.[8] Indeed, even some gas-phase proton-transfer reactions of hydrocarbon radical cations involve the formation of metastable complexes, for example, the reaction of cyclohexane$^{\bullet+}$ with water.[17] Furthermore, the complexation may account for other "puzzling" observations[18,19] (see part 2 of this series).[20]

Recently, we found an example of the complexation in a reaction of *trans*-decalin$^{\bullet+}$ with 2-propanol.[14] It was found that the scavenging kinetics observed at room temperature was biexponential. This bimodality was explained through the formation of a complex with a lifetime of 30 ns. In this work, we study the scavenging of decalin holes by a number of aliphatic alcohols. It is shown that all such reactions proceed through the formation of a complex. The equilibrium constant of the complexation varies 2−3 orders of magnitude, depending on the solute structure and the solvent temperature. In *cis*-decalin, the complexes are more stable than those in *trans*-decalin, which explains the observations of Sauer et al.[10] Together with part 2 of this series,[20] our study suggests that *all* proton-transfer reactions of cycloalkane holes proceed through complex formation.

2. Scavenging Kinetics

2.1. Hole Injection. In this work, hole injection was used as the source of free solvent holes. Decalin holes ($C_{10}H_{18}^{\bullet+}$) were produced by rapid transfer of the solvent valence electron to the photoexcited radical cation of triphenylene$^{\bullet+}$:

$$\text{triphenylene}^{\bullet+} + h\nu \rightarrow \text{triphenylene}^{\bullet+}* \qquad (1)$$

$$\text{triphenylene}^{\bullet+}* + C_{10}H_{18} \rightarrow \text{triphenylene} + C_{10}H_{18}^{\bullet+} \qquad (2)$$

Triphenylene$^{\bullet+}$ was generated by ionization of its parent molecule using a 5 eV laser pulse. Reaction (1) was initiated by a 2.33 eV pulse triggered at $t = t_d$ after the 5 eV pulse (Figure 1); time t_d was varied between 1 and 10 μs. At these delay times, the geminate recombination is over and the ions slowly recombine in the solvent bulk. Triphenylene was used because its radical cation has strong absorbance at 2.33 eV ($\epsilon_{532} \approx 2.7 \times 10^3$ M^{-1} cm^{-1})[14] and exhibits a high yield of hole injection at laser fluences ~ 1 J/cm^2 (the quantum yield is $(4.6 \pm 0.3) \times 10^{-2}$ per 2.33 eV photon).[14] For triphenylene$^{\bullet+}$, reaction (1) is single-photon and reaction (2) is very fast ($\approx$9.5 ps).[22]

The sequence of photolytic and chemical events is as follows: 5 eV laser excitation of triphenylene yields the singlet excited state; this state absorbs the second 5 eV photon and autoionizes, yielding a geminate pair of triphenylene$^{\bullet+}$ and solvated electron. The latter is rapidly scavenged by CO_2 (added as a scavenger), yielding the $CO_2^{\bullet-}$ anion. Some triphenylene$^{\bullet+}$ cations absorb the 5 eV photon, yielding decalin$^{\bullet+}$ via reaction (2) (with quantum yield >0.16/5 eV photon).[14] At $t_d > 1-3$ μs, essentially all of the geminate pairs have recombined, and 4−5% of the initial ions have escaped each other's attraction (so-called "free ions"). Within the same time period, solvent holes generated by the 5 eV pulse decay in reactions with the solute and impurity. The residual dc conductivity signal is due to 0.01−0.3 μM of free molecular ions whose recombination occurs on the time scale of milliseconds.

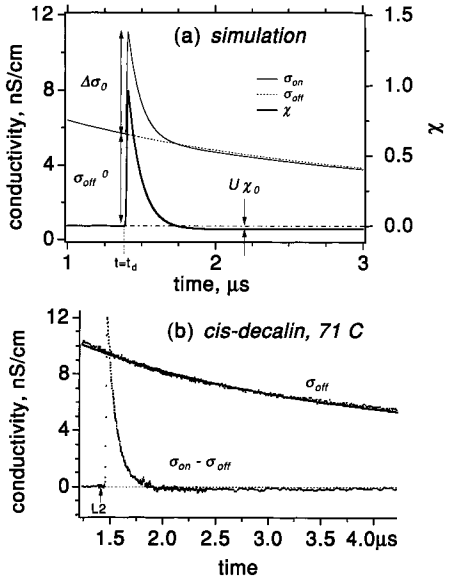

Figure 1. (a) Simulated kinetics of photoinduced dc conductivity (see part 1 in the Supporting Information for more details). The simulation parameters ($\mu_h = 2.95 \times 10^{-7}$ m^2 V^{-1} s^{-1}, $\nu = 3.1$, $k_1 = 10^7$ s^{-1}, $C_0 = 0.84$ μM, $f_h = 0.42$, $\epsilon = 2.14$, and $t_p = 6$ ns) were chosen to simulate scavenging kinetics shown in (b). The conductivity is given in the units of nS/cm ($=10^{-7}$ Ω^{-1} m^{-1}). The 2.33 eV laser pulse is triggered at $t_d = 1.4$ μs. The bold line is the χ kinetics, the thin line is the σ_{on} kinetics, and dashed line is the σ_{off} kinetics. The undershoot is $\approx 2.1 \times 10^{-2}$ (see the Supporting Information). (b) Experimental σ_{off} and $\Delta\sigma$ signals from a CO_2-saturated solution of 15 μM triphenylene in *cis*-decalin at 71 °C. The σ_{off} kinetics is fit (solid line) by second-order dependence. Note the undershoot in the $\Delta\sigma$ kinetics.

SCHEME 1

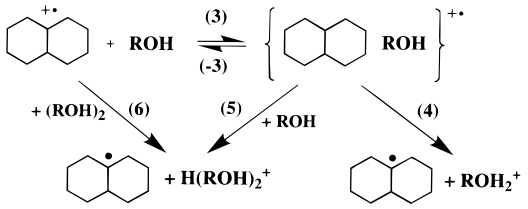

2.2. The Complexation (Scheme 1). For alcohols (ROH), the scavenging kinetics of the solvent holes were biexponential (see, for example, Figures 2 and 3). These kinetics may be simulated using the kinetic model shown in Scheme 1 (reactions 3−6).

In this scheme, a reactive encounter of the solvent hole with a ROH molecule, reaction (3) (with rate constant k_3), yields complex C^+. This complex dissociates with rate constant k_{-3}

The efficiency of hole injection was quantified by comparing signals of the 2.33 eV photoinduced conductivity $\Delta\sigma = \sigma_{on} - \sigma_{off}$ and of the 5 eV photoinduced free ions (σ_{off}), as shown in Figure 1. If one neglects the increased bimolecular recombination immediately after the hole injection (the limits of this assumption are examined in part 1 of the Supporting Information), the quantity $\chi(t) = \Delta\sigma/\sigma_{off}$ is directly proportional to the concentration of photoinduced solvent holes.

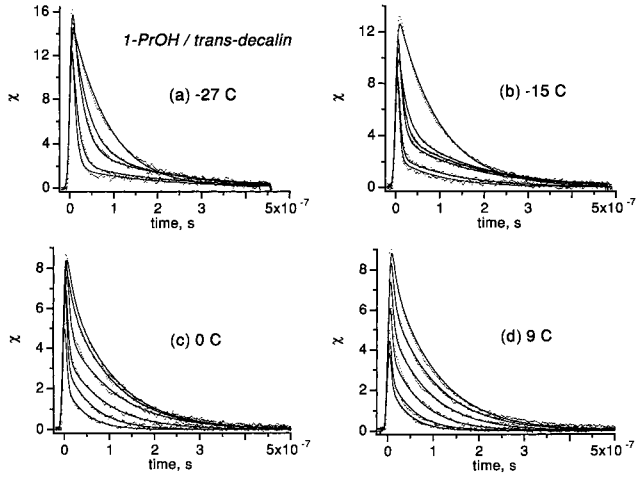

Figure 2. Decay kinetics χ for the scavenging of solvent holes in *trans*-decalin by 1-propanol as a function of temperature. Dots are experimental; solid lines are simulations using multitrace least-squares fitting with eq 9; the kinetics were convoluted with the Gaussian time profile of the 2.33 eV laser (6 ns fwhm). Solute concentrations for each trace are given in Table 4S. See Figure 6 and Tables 2 and 3 for kinetic parameters.

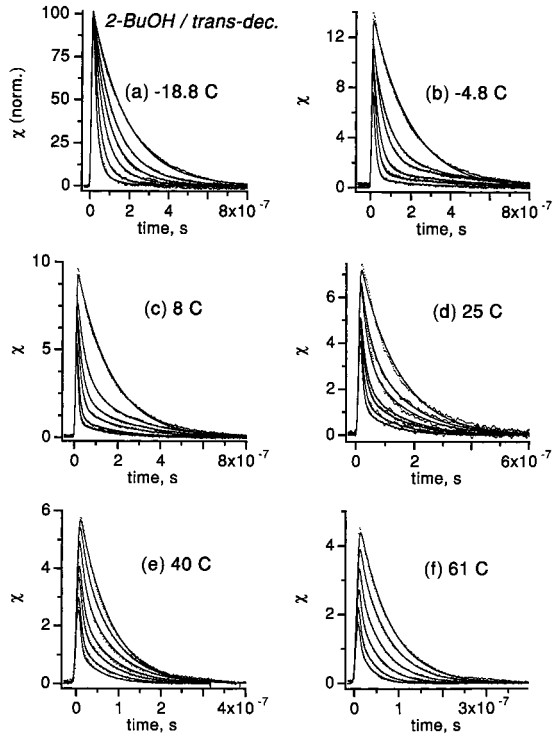

Figure 3. Same as Figure 2, for 2-butanol in *trans*-decalin. See Figure 6 and Tables 2 and 3 for kinetic parameters. Kinetics in segment (a) are normalized at the maximum of the signal.

(so that the equilibrium constant of the complexation $K_{eq} = k_3/k_{-3}$) or decays by proton-transfer reactions (4) and (5). This transfer may occur either within the complex (rate constant k_4) or after the encounter with another ROH molecule (rate constant k_5). The solvent hole may also decay in reaction with impurity (with rate constant k_0, not shown in the scheme). The latter would include the decay of the solvent hole by charge neutralization (see above). Reaction (6) with alcohol clusters[26,27] is discussed in the Supporting Information. When the stated assumptions are used, the kinetics are given by

$$d[H^+]/d\tau = -(r_1 + r_3)[H^+] + r_2[C^+] \quad (7)$$

$$d[C^+]/d\tau = r_1[H^+] - (r_2 + r_4)[C^+] \quad (8)$$

where τ is the delay time after the 2.33 eV laser pulse, $[H^+]$ is the concentration of solvent holes, $r_1 = k_3[ROH]$, $r_2 = k_{-3}$, $r_3 = k_0$, and $r_4 = k_4 + k_5[ROH]$. Solving eqs 7 and 8 and assuming that the complex exhibits normal mobility, one obtains

$$\chi(\tau)/\chi(\tau{=}0) = \beta f(\lambda_1;\tau) + (1-\beta) f(\lambda_2;\tau) \quad (9)$$

$$\beta = (r_2 + r_4 - \lambda_1)/\Delta \quad (10)$$

$$\lambda_{2,1} = (r \pm \Delta)/2 \quad (11)$$

where $\Delta^2 = r^2 - 4(r_2 r_3 + r_3 r_4 + r_4 r_1)$ and $r = \sum_i r_i$. Function $f(\lambda;\tau)$ in eq 9 is $\exp(-\lambda t)$ convoluted with the temporal profile of the 2.33 eV laser pulse (see eq 7S in the Supporting Information). For $\lambda_2 \gg t_p^{-1}$, the equilibrium is reached "instantaneously" and

$$\chi(\tau) \propto \exp(-k_1\tau) \quad (12)$$

where

$$k_1 \approx \{k_0 + (k_4 + k_5[ROH])K_{eq}[ROH]\}/(1 + K_{eq}[ROH]) \quad (13)$$

Thus, even when the kinetics are "monoexponential", the complexation may be observed through nonlinear dependence of k_1 on [ROH] (as in Figure 4). In our experiments, the onset of the "monoexponential" kinetics was at $K_{eq} \sim 10^3$ M^{-1}. Though some rate constants may be determined, even for lower K_{eq} (from the dependence of k_1 vs [ROH], eq 13), we preferred to analyze the kinetics that exhibited clear bimodal behavior, which occurred for K_{eq} between 10^3 and 3×10^4 M^{-1}. Typically, a family of $\chi(t)$ kinetics (corresponding to 5−10 concentrations of the solute) were analyzed simultaneously using eq 9 and the optimum set of rate constants (k_0, k_3, k_{-3}, k_4, and k_5) was obtained from the least-squares fit; the optimum $\chi(\tau{=}0)$ values were determined for each of these kinetics separately.

This fitting procedure did not always give unique values for the rate constants k_4 and k_5. For $K_{eq} > 10^4$ M^{-1}, the complex mainly decays by reaction (4) and the fitting procedure is not sensitive to k_5. For $K_{eq} \sim 10^3$ M^{-1}, the opposite is true. Generally, we separated reactions (4) and (5) by studying the temperature dependence of the kinetics; however, in several cases this was not possible and we assumed $k_5 = 0$. Fortunately, optimum values of k_3 and k_{-3} are almost independent of the k_4/k_5 ratio. For ethanol, reaction (4) was not necessary to simulate the kinetics. Complications caused by association of alcohol molecules in low-temperature cycloalkanes are discussed in part 2 of the Supporting Information.

2.3. Justification of the Model. Because the lifetime of C^+, as determined from our experiments, is relatively long (Table 2), reaction (4) must be relatively inefficient. Only when a second ROH molecule encounters the complex does the proton transfer occur rapidly. Such a situation is possible if the exothermicity of the net reaction

$$C_{10}H_{18}^{\bullet+} + ROH \rightarrow C_{10}H_{17}^{\bullet} + ROH_2^+ \quad (14)$$

is not greater than the binding energy of the complex.

Using the IP_g of *trans*-decalin (9.25 eV),[16] the gas-phase proton affinity (PA_g) of *trans*-decalyl radicals may be estimated as 4.35 eV + D_{C-H}, where the D_{C-H} is the C−H bond dissociation energy. Depending on the position of free valence

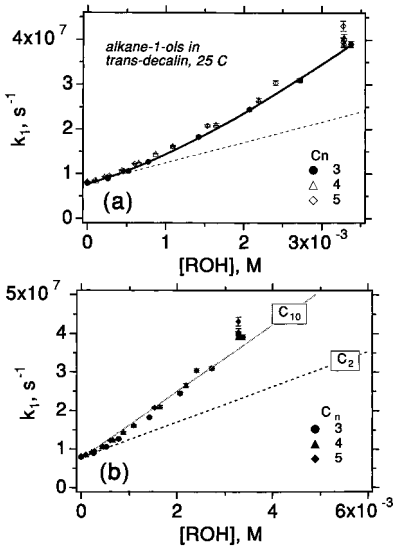

Figure 4. (a,b) Concentration dependence of the pseudo-first-order rate constant k_1 for the scavenging of *trans*-decalin$^{\bullet+}$ by C_2-C_{10} primary alcohols at 25 °C. The data are plotted twice to emphasize the superlinearity of concentration plots for C_3-C_5 alcohols. For ethanol (dashed line) and decanol (dotted line), the dependencies are linear (the data points are shown in the Supporting Information, Figure 12S-(a)); for propanol, butanol, and pentanol the dependencies are curved (see the text and eq 13).

TABLE 2: Rate Constants for Scavenging of *trans*-Decalin$^{\bullet+}$ by Aliphatic Alcohols at 25 °C[a]

solute	$k_3 \times 10^{11}$, M^{-1} s^{-1}	$k_{-3} \times 10^6$, s^{-1}	$k_4 \times 10^6$, s^{-1}	$K_{eq} \times 10^3$, M^{-1}	τ_c[b], ns
2-propanol	1.18 ± 0.04	30 ± 1	11 ± 0.2	3.92	24
2-butanol	0.94 ± 0.02	15 ± 0.04	7.4 ± 0.12	6.2	45
3-pentanol	1.17 ± 0.02	15 ± 0.3	8.9 ± 0.12	7.9	42
cyclohexanol	1.26 ± 0.01	6.7 ± 0.1	6.3 ± 0.1	18.8	77
tert-butanol	1.12 ± 0.01	3.7 ± 0.16	7.5 ± 0.3	30	89

[a] The scavenging kinetics were fit assuming $k_5 = 0$; error limits correspond to the 90% confidence obtained from a multitrace least-squares fit. [b] $\tau_c = 1/(k_{-3} + k_4)$ is the natural lifetime of the complex.

in the decalyl radical, the estimated D_{C-H} varies from 3.55 to 4.1 eV,[23] which yields PA_g between 7.9 eV (for the 9-decalyl radical) to 8.45 eV (for the spin at other positions). PA_g for the monomers of ethanol and 2-propanol are 8.18 and 8.3 eV, respectively.[24] Dimerization of ROH molecules increases these affinities by at least 1 eV, making the proton transfer very efficient. (For methanol, dimerization increases the proton affinity by 1.3 eV).[25] Thus, we expect that reaction (5) is diffusion-controlled.

We used semiempirical AM1 calculations to estimate the heats of gas-phase reactions (3) and (14). For reaction (14), the values obtained are −0.17 eV for ethanol, −0.19 eV for 1-propanol, and −0.43 eV for 2-propanol (*trans*-decalin). For methanol, reaction (14) is calculated to be endothermic by 0.1 eV. According to these calculations, the complex is bound by weak interaction of the hydroxyl group and three axial hydrogens (H_{ax}) of the *trans*-decalin radical cation. In the optimum geometry, the oxygen is above the center of a triangle formed by H_4, H_5, and H_9 axial hydrogens; the hydroxyl proton looks away from this plane; the shortest $H_{ax}-O$ distance is 0.23 nm. In this structure, >95% of the positive charge is on *trans*-decalin; the binding energy varies from 46 kJ/mol for methanol to 38 kJ/mol for 2-butanol. These estimates compare favorably with the experimental heats of complexation (Table 3). In conclusion, our estimates suggest that reaction (3) is energetically preferable to reaction (14).

TABLE 3: Summary of the Activation Energies and Equilibrium Parameters for Complexation of Decalin Holes by Aliphatic Alcohols

solute	T, °C[d]	E_a for k_4 (k_5)[e]	$-\Delta H°$ [f]	$-\Delta G°$ [f]	$-\Delta S°$ [g]
1-propanol[a]	−27 to +8	11.8 ± 3.6	38 ± 3	15 ± 6	77 ± 12
2-propanol[a]	−29 to +41		34 ± 2	20 ± 5	49 ± 8
2-butanol[a,c]	−19 to +61	26.6 ± 0.5	30 ± 0.5	21 ± 1	29 ± 1.5
tert-butanol[a,c]	+25 to +80	22.7 ± 3	25 ± 2	25 ± 4	0 ± 7
ethanol[b]	+25 to +71	24.8 ± 3.4	39.7 ± 1	25 ± 2.5	49.5 ± 4

[a] *trans*-Decalin. [b] *cis*-Decalin; assuming $k_4 = 0$. [c] Assuming $k_5 = 0$. [d] Temperature interval of the measurement. [e] Activation energy, kJ/mol. [f] Standard potential at 298 K, kJ/mol. [g] Standard entropy at 298 K, J mol^{-1} K^{-1}.

3. Experimental Section

Materials. *trans*-Decalin and UV-grade alcohols were obtained from Aldrich; *cis*-decalin was obtained from Chemsampco (formerly, Wiley Organics). The decalin solvents were purified by multiple passage through 1-m silica gel columns. After the purification, the decalins contained 1−2% of the isomer, 0.5−1% of cyclohexane and 3-methylpentane, 0.1−0.5% of methylcyclohexane, and traces of higher hydrocarbons (such as perhydroindenes). With exception of cyclohexanol (that was purified by addition of activated charcoal), the alcohols were used without purification. If not stated otherwise, the solute concentrations are given in mol dm^{-3} (M) at 25 °C (even when the measurements were carried out at other temperatures). Alcohols are very volatile, and the concentration drops during purging of the decalin solutions with CO_2. For that reason, the solutions were saturated with CO_2 prior to the addition of the solute. No reliable measurement for methanol was possible due to its low miscibility with decalins.

Laser Conductivity Apparatus. A 20-ns fwhm pulse of 5 eV photons (0.1 J/cm^2) from a Lambda Physik LPX 120i laser was used to ionize 10−15 μM of triphenylene in CO_2-saturated decalin. A 2.33 eV (second harmonic) pulse from a Continuum model 8010 laser (0.85 J/cm^2) was applied to photoexcite triphenylene$^{\bullet+}$. The lasers were operated at 1 Hz, and the delay times between the laser pulses were controlled with accuracy to ±3 ns. If not stated otherwise, the delay time t_d of the 2.33 eV pulse was 1 μs for *trans*-decalin and 2.96 μs for *cis*-decalin. The 2.33- and 5 eV beams were coincident inside a conductivity cell with 0.6-cm spacing between the electrodes. The 5 eV beam passed through an aperture at the front of the cell and the 2.33 eV beam entered through an aperture at the rear. Circular apertures 0.4 cm in diameter were used for *trans*-decalin and rectangular 0.4 × 0.7 cm apertures were used for *cis*-decalin.

Conductivity cells with optical paths of 1 cm (*trans*-decalin) or 2 cm (*cis*-decalin) were used, and the field between the electrodes was 6.7 kV/cm. The cell body was made of machinable ceramic; suprasil windows were cemented using Torr-Seal epoxy (Varian). The cell was placed in an aluminum jacket that served as a heat exchanger. Cold *n*-hexane (−45 to 25 °C) was circulated through the jacket using a FMS Systems model MC880A1 cryogenic bath equipped with a pump. To obtain temperatures from 25 to 90 °C, hot water was circulated instead; cartridge electric heaters were used above 90 °C. The temperature inside the cell was calibrated using a thermocouple probe inserted between the electrodes; this probe was removed during the photoconductivity measurement; the readings in the cell were within ±1 °C of the temperature of the jacket.

The photocurrent through 50 Ω was amplified 100 times using two CLC449 amplifiers; the signal was acquired with a DSA-601 digitizer. The cell was enclosed in an aluminum box that shielded it from electromagnetic interference produced by the

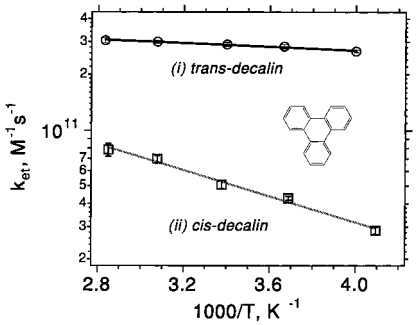

Figure 5. Arrhenius plot for rate constants k_{et} for electron transfer from triphenylene to the solvent hole in (i) *trans*- and (ii) *cis*-decalins. The solute concentrations were corrected for the solvent expansion (Table 1). The activation energies are given in Table 1.

lasers. Weak signals from the 2.33 eV pulses alone (observed only within the duration of the laser pulse) were subtracted from each σ_{on} trace.

Two methods were used to account for the effect of ion recombination in the kinetic analyses (see part 1 of the Supporting Information). With the first method, the 2.33 eV pulse was fired for every second 5 eV pulse, and the σ_{on} and $\sigma_{off} - \sigma_{on}$ kinetics were collected separately (as in Figure 1b). The σ_{off} kinetics were smoothed and $\chi(t)$ was obtained. With the second method the "tail" of the σ_{on} trace was fit with a second-order kinetics and back extrapolated to $t = 0$ (yielding σ_{off}); the $\chi(t)$ trace was obtained from the extrapolated σ_{off} curves. We mainly relied on the latter method, using the former one to estimate the undershoot (shown in Figure 1).

Only a few examples of the $\chi(t)$ kinetics (Figures 2 and 3) and Arrhenius plots for rate constants (Figure 6) are given in the article. We refer the reader to the Supporting Information for more data. In particular, solute concentrations for kinetics shown in Figures 2 and 3 are listed in Table 4S therein. Figures 9−16, which are referred to with designator "S" after the number (e.g., Figure 9S), are also placed in the Supporting Information.

4. Results and Discussion

4.1. Temperature Dependence of Electron-Transfer Rates. The rate constants, k_{et}, for electron-transfer reactions of decalin holes give an estimate of the upper limit for the complexation rates. The temperature dependence of k_{et} had been reported in ref 11. In that work, the fluence of 2.33 eV photons was only one-fifth of that employed in our study, and the signal-to-noise ratio was 10−20 times worse than that obtained using the present setup. For this reason, the distortion of the kinetics due to charge recombination (see the Supporting Information) was not noticed and no provision was made to compensate for it. Using the improved analyses, we obtained more reliable data on the rate constants, k_{et}, for the scavenging of *cis*- and *trans*-decalin holes by triphenylene ($IP_g \approx 7.84$ eV). The scavenging kinetics were pseudo-first-order, and bimolecular rate constants of electron transfer, k_{et} (Figure 5), were determined from the concentration dependencies of k_1. As shown in Table 1, the activation energies for the electron transfer are close to the activation energies of the hole migration. (This correspondence was not observed in the previous measurement.[11]) We conclude that rapid electron-transfer reactions are diffusion-controlled.

4.2. Reactions with Alcohols at Room Temperature. Room-temperature kinetics for reactions of decalin holes with alcohols could be divided into three classes: Class-I kinetics were "monoexponential"; the pseudo-first-order rate constants k_1 showed linear dependence on [ROH] (Figure 13S(a)). Class-II

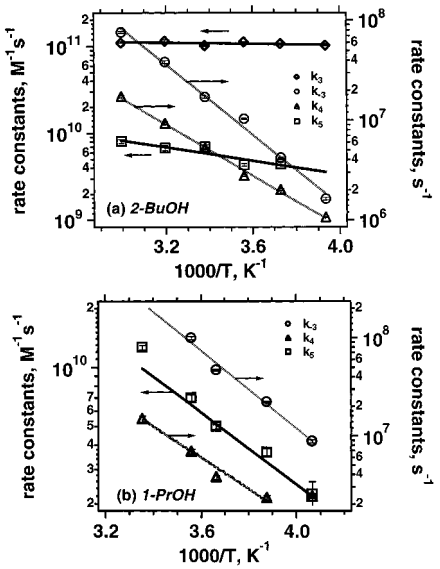

Figure 6. Arrhenius plots for rate constants of reactions (3)−(5) for (a) 2-butanol (Figure 3) and (b) 1-propanol (Figure 2) in *trans*-decalin. Note the weak temperature dependence of k_3 for 2-butanol; for 1-propanol, the kinetics were fit assuming $k_3 = 1.1 \times 10^{11}$ M^{-1} s^{-1} over the entire temperature range.

kinetics were also "monoexponential", but k_1 did not increase linearly with [ROH] (Figure 4). Instead, the increase in k_1 with increasing [ROH] was superlinear. This type of behavior is consistent with that given by eq 13. Class-III kinetics were biexponential (e.g., Figure 3d).

In room temperature *trans*-decalin, class-I kinetics were observed for ethanol and 1-decanol (Figures 13S(a)). In *cis*-decalin at room temperature, all alcohols that were examined exhibited such kinetics. This would happen in two extremes: (i) very strong complexation ($K_{eq} > 10^4$ M^{-1}) or (ii) very weak complexation ($K_{eq} < 10^2$ M^{-1}). In the first case, increasing the temperature reduces the stability of the complex, and the kinetics changes to class II or class III. For example, 2-propanol in *cis*-decalin exhibited class-I behavior below 70 °C and class-II behavior above 70 °C. Though the nonlinearity in the concentration dependence of k_1 was barely discernible, even at 110 °C, the complex mechanism of the scavenging reaction manifested itself through non-Arrhenius behavior of the scavenging constants k_2 (Figure 9S). Fitting the 78 °C kinetics with eq 9 suggested the occurrence of the complexation with $k_3 \approx 3.2 \times 10^{10}$ M^{-1} s^{-1} and $K_{eq} \approx 7800$ M^{-1}. For other alcohols in *cis*-decalin, the scavenging constants k_2 (determined by linearization of the concentration plots for k_1) also pass through a maximum. For ethanol, this maximum was attained at 40 °C (Figure 9S). Again, fitting the kinetics with eq 9 indicated bimodality with an equilibrium constant, K_{eq}, that varied between 3000 M^{-1} at 70 °C and $(1-2) \times 10^4$ at 40 °C (Table 3 and Figures 15S and 16S). This and other results suggest that in room-temperature *cis*-decalin, $K_{eq} > 10^4$ M^{-1} for all alcohols. Because the equilibrium (3) is shifted toward complex formation, scavenging constants k_2 extracted from single-exponential fits are all similar: $(2.09 \pm 0.14) \times 10^{10}$ M^{-1} s^{-1} for ethanol, $(2.23 \pm 0.06) \times 10^{10}$ M^{-1} s^{-1} for 1-propanol, and $(2.13 \pm 0.3) \times 10^{10}$ M^{-1} s^{-1} for 2-propanol.

In *trans*-decalin, class-I, case (i) kinetics were observed for all branched alcohols at very low temperature, that is, the case where the complexes become stable on the time scale of the observation. In this regime, rate constants k_2 rapidly increase with decreasing temperature, eventually approaching $k_3 \approx 1.1$

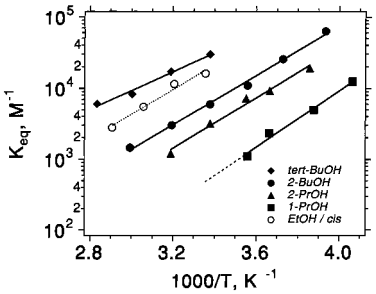

Figure 7. The van't Hoff plots for the equilibrium constants of complexation reaction (3) for *cis*-decalin$^{\bullet+}$ with ethanol (empty circles) and *trans*-decalin$^{\bullet+}$ with *tert*-butanol (filled rhombs), 2-butanol (filled circles), 2-propanol (filled triangles), and 1-propanol (filled squares).

$\times 10^{11}$ M^{-1} s^{-1} (e.g., for *tert*-butanol in −19 °C *trans*-decalin, $k_2 \approx 8.5 \times 10^{10}$ M^{-1} s^{-1}).

In case (ii), cooling the reaction mixture has the same effect as warming it in case (i); for example, for ethanol in *trans*-decalin, class-I kinetics were observed down to −15 °C. Only at −26 °C did we observe bimodal scavenging. These low-temperature kinetics were fit using eq 9 to obtain $K_{eq} \approx 1570$ M^{-1} (Figure 13S(b)). For comparison, 1-propanol exhibits $K_{eq} \approx (1.1-1.2) \times 10^4$ M^{-1} under the same conditions (Figures 6b and 7). Apparently, ethanol forms less stable complexes than higher alcohols. Interestingly, in room-temperature *trans*-decalin, ethanol scavenges solvent holes with rate constant of $(4.6 \pm 1) \times 10^9$ M^{-1} s^{-1}, while 1-decanol exhibits a rate constant twice as large, $(8.7 \pm 0.1) \times 10^9$ M^{-1} s^{-1}. The lower rate is due to inability of the monomer of ethanol to accept the proton from *trans*-decalin$^{\bullet+}$.

We turn now to class-II kinetics exhibited, for example, by 1-propanol, 1-butanol, and 1-pentanol in the room-temperature *trans*-decalin (Figure 4a). At lower concentrations of alcohol ([ROH] < 0.5 mM, Figure 4a), the scavenging constant is $\approx 5 \times 10^9$ M^{-1} s^{-1} (comparable to that observed for ethanol, Figure 13S(a)), while at higher concentrations the rate constant is $(9.3 \pm 0.4) \times 10^9$ M^{-1} s^{-1} (which is close to that observed for 1-decanol, Figures 4b and 13S(a)). The overall concentration dependence may be fit using eq 13, though there is no unique set of parameters K_{eq}, k_4, and k_5 that fits the kinetic data. For 1-propanol, the least-squares fit shown in Figure 4b yields $K_{eq} \approx 200$ M^{-1}, $k_4 \approx 3.6 \times 10^7$ s^{-1}, and $k_5 \approx 1.7 \times 10^{10}$ M^{-1} s^{-1}. Extrapolation from the low-temperature data of Figures 2 and 6 (below the onset of class-III kinetics) suggest that $K_{eq} \approx 480$ M^{-1} at 25 °C (Figure 7). In other cases when class-II kinetics were observed, K_{eq} also was between 200 and 1000 M^{-1}.

Class-III kinetics are the simplest to interpret. Only secondary and ternary alcohols exhibited such kinetics at 25 °C in *trans*-decalin (Table 2 and Figures 3d, 11S(a), and 12S). In *cis*-decalin, class-III kinetics were observed for one solute only, ethanol (Figure 14S).

Because only stable complexes exhibit bimodal kinetics at 25 °C ($K_{eq} > 4 \times 10^3$ M^{-1}), reaction (5) does not occur at low concentrations of the solute (<1 mM), and we let $k_5 = 0$ in our analyses. The optimum parameters found from the least-squares fits using eq 9 are given in Table 2. The stability and lifetimes τ_c of the complexes systematically increase with the carbon number and are higher for tertiary alcohols. The complexation constant K_{eq} increases from 3.9×10^3 M^{-1} for 2-propanol to 3×10^4 M^{-1} for *tert*-butanol; the natural lifetime τ_c of the complex (defined as $\tau_c^{-1} = k_{-3} + k_4$) increases from 25 to 90 ns (Table 2). By contrast, for solutes demonstrating class-II kinetics at 25 °C, the lifetime is just a few nanoseconds. The rate constant of complexation, reaction (3), varies little among the solutes, $k_3 \approx (1-1.25) \times 10^{11}$ M^{-1} s^{-1}. This constant is approximately one-third of the rate constant for electron-transfer reactions in *trans*-decalin. The rate constant k_4 also varies little, $k_4 \approx (5-10) \times 10^6$ M^{-1} s^{-1}. The slowness of reaction (4) indicates that the complexation is favored energetically over reaction (14), as discussed in section 2.3.

4.3. Temperature Dependencies. In this work, a primary objective was to obtain temperature dependencies of the equilibrium constants K_{eq} to determine thermodynamic potentials for complexation. Therefore, we were limited to a few alcohols that exhibit class-III kinetics over a sufficiently wide temperature range (Table 3). Ultimately, we chose the five alcohols listed in Table 3. The sets of $\chi(t)$ kinetics for each temperature were fit separately; no global fits were attempted. The following trends were observed:

(a) In *trans*-decalin, the complexation rate constant k_3 was almost temperature-independent. The estimates for the activation energy of reaction (3) varied between 0 ± 0.7 kJ/mol for 2-butanol (Figures 3 and 6) and 2.7 ± 0.7 kJ/mol for 2-propanol (Figures 10S and 15S). Actually, these kinetics can be equally well fit assuming that $k_3 \approx (1.1-1.2) \times 10^{11}$ M^{-1} s^{-1} at any temperature. Given that electron-transfer reactions of solvent holes in *trans*-decalin are also thermoneutral (Table 1), we believe that the complexation is diffusion-controlled in the entire liquid range. On the basis of the results of k_3 and values of μ_h from Table 1, the reaction radius R_c of the complexation is estimated to be between 0.65 and 0.73 nm (depending on temperature). In comparison, on the basis of data of gas-phase molecular volumes,[28] the radii of *trans*-decalin and butanols are estimated as 0.47 and 0.37 nm, respectively, which gives an estimate of $R_c \approx 0.85$ nm for the reaction radius.

(b) For ethanol in *cis*-decalin, the optimum rate constants k_3 were also temperature-independent ($\approx 3 \times 10^{10}$ M^{-1} s^{-1} between 25 and 80 °C; see Figures 14S and 16S). In this solvent, the electron transfer at 80 °C is 50% faster than that at 25 °C (Figure 5 and Table 1). Therefore, the complexation of ethanol with *cis*-decalin$^{\bullet+}$ is not diffusion-controlled (for reaction of ethanol with *trans*-decalin$^{\bullet+}$ we also observed a reduced rate of complexation, see the caption to Figure 13S(b)). At 25 °C, the complexation is quite efficient because its rate is ≈60% of the electron-transfer rate. Using the data of Table 1, we estimate $R_c \approx 0.79$ nm. van der Waals radii of *cis*-decalin and ethanol are 0.482 and 0.322 nm, respectively,[28] which gives the estimate $R_c \approx 0.804$ nm, in good agreement with the experiment.

(c) Where the rate constant k_4 could be determined, the activation energy of proton transfer is 10−25 kJ/mol, for both decalins. This high barrier explains the relative stability of the complex. Where the rate constant k_5 could be determined, the activation energy of proton transfer is comparable to $E_a(\mu_i)$ (Table 1) and is different for *cis*- and *trans*-decalins. These rate constants are close to those for diffusion-controlled reactions of normally migrating species. Where the first- and second-order proton transfers were kinetically separable, the k_4/k_5 ratio was between 0.5 and 2 mM.

4.4. Thermodynamics. Standard free energy $\Delta G°$,

$$\Delta G° = \Delta H° - T\Delta S° \qquad (15)$$

enthalpy $\Delta H°$, and entropy $\Delta S°$ of reaction (3) at 25 °C were obtained from van't Hoff plots shown in Figure 7. Figure 8 exhibits the plots of $\Delta G°$ and $\Delta S°$ as a function of the reaction heat $\Delta H°$. Several conclusions can be drawn from examination of the results in Table 3 and Figure 8:

(a) The standard heat of the complexation systematically decreases with the carbon number of the alcohol (≈3−5 kJ/

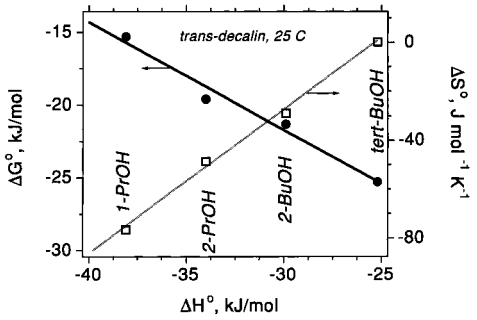

Figure 8. A correlation between the standard enthalpy, driving force, and entropy of reaction (3) in *trans*-decalin. See also Table 3.

mol per carbon atom) and the degree of derivatization. These trends are in agreement with the gas-phase calculations (section 2.3).

(b) There is an anticorrelation between the $\Delta G°$ and $\Delta H°$ (Figure 8): *weaker* bound complexes are *more* stable. This anticorrelation is due to a systematic increase in the standard entropy $\Delta S°$ of reaction (3) with $\Delta H°$. For ethanol in *cis*-decalin and 1-propanol in *trans*-decalin, $-\Delta S°$ is $\approx$ 80 J mol^{-1} K^{-1}, while for *tert*-butanol $\Delta S° \approx 0$. The entropic factor is predominant in determining the stability of the complex at 25 °C.

(c) Assuming that the heat of reaction (3) is similar for both decalins and extrapolating the linear dependencies in Figure 8, we estimated that the driving force $\Delta G°$ of complexation in *cis*-decalin is $\approx$10 kJ/mol lower than that in *trans*-decalin. In such a case, the driving force $\Delta G°$ of reaction (3) in *cis*-decalin must be between $-$25 kJ/mol (1-propanol) and $-$35 kJ/mol (*tert*-butanol), which corresponds to K_{eq} between 2×10^4 and 1.5×10^6 M^{-1} at 25 °C. These estimates indicate that for complexes of *cis*-decalin with higher alcohols $\Delta S°$ is $\approx$35 J mol^{-1} K^{-1} more positive than $\Delta S°$ for complexes of *trans*-decalin. This means that, for butanols in *cis*-decalin, $\Delta S°$ is *positive*. For complexation of *trans*- and *cis*-decalin holes with benzene (see part II of this series),[20] we obtained $\Delta S°$ of $-(31.6 \pm 9.6)$ and $+(3 \pm 4.4)$ J mol^{-1} K^{-1}, respectively. Once more, in *cis*-decalin, the entropy was $\approx$35 J mol^{-1} K^{-1} higher and $\Delta S°$ was positive within the accuracy of the measurement.

Given the extreme stability and low heat of reaction (3) for higher alcohols in *cis*-decalin, it is not surprising that the decay kinetics of solvent holes is "monoexponential" up to 110 °C. This efficient complexation would account for higher scavenging rate constants in this solvent as compared to those in *trans*-decalin (in which the complexes are less stable).

4.5. Entropy of Complexation. A linear correlation between the heat and entropy of complexation is common for many molecular complexes, such as donor$-$acceptor[29] and hydrogen-bonded[30] complexes. Though there is no rigorous theory concerning this correlation, it is intuitively reasonable: the weaker the interaction between the complexants, the more degrees of freedom are preserved in the complex. For complexes of *trans*-decalin$^{\bullet+}$ with aliphatic alcohols, the slope of $\Delta H°$ versus $\Delta S°$ is $\approx 170 \pm 10$ K which is comparable to that for hydrogen-bonded complexes in nonpolar liquids (between 200 and 260 K per bond).[30] What seems surprising is that the entropy of reaction (3) is so low (approaching zero for higher alcohols in *trans*-decalin). As was argued above, for higher alcohols in *cis*-decalin, $\Delta S°$ is *positive*. Such behavior is unprecedented for molecular complexes: complexation always reduces the degrees of freedom in the complexants so that $\Delta S° < 0$. On the other hand, positive $\Delta S°$ is typical for reactions of ligand exchange. Consider, for example, a hypothetical reaction

$$C_{10}H_{18}{}^{\bullet+} + (ROH)_2 \rightarrow (C_{10}H_{18}\,ROH)^{\bullet+} + ROH \quad (16)$$

Because one of the ROH molecules gains degrees of freedom, the net change in the entropy could be positive. Of course, reaction (16) is very unlikely: As explained in the Supporting Information, at elevated temperatures there are too few dimers to scavenge the holes and, in any case, an encounter with the dimer would likely result in rapid proton transfer, reaction (6). The only way to account for positive (or near-zero) entropy in reaction (3) is to postulate that the *solvent itself* gains degrees of freedom upon complexation.

This brings us to the nature of solvent holes in cycloalkane liquids. There are two schools of thought about these species.[1,2] The predominant view is that the solvent holes are radical cations of hydrocarbons. The charge is localized on a given molecule and occasionally hops to the nearest neighbor. The principal difficulty with this concept is that it does not account for high hopping rates, low transport barriers, and significant delocalization of solvent holes in the four cycloalkanes exhibiting long-lived high-mobility holes.[1−3,5,11] The alternative view is that the hole is a small polaron in which the positive charge is shared by several solvent molecules.[1,5,11] If the latter view is correct, reaction (3) should be written as

$$Sol_n{}^{\bullet+} + ROH \rightarrow \{Sol^{\bullet+} \ldots ROH\} + (n-1)Sol \quad (17)$$

where Sol stands for solvent molecule and $Sol_n{}^{\bullet+}$ for polaron delocalized over n such molecules. Reaction (17) may be viewed as a ligand exchange around the hole. Because reaction (17) restores degrees of freedom to the solvent molecules, its entropy could be positive.

We may crudely estimate the effect of the solvation on the energetics of reaction (3) in a dielectric continuum model. In this model, the driving force ΔG_s^0 and entropy of ion solvation are given by

$$\Delta G°_s = e^2/2r_+(1-\epsilon^{-1}) \quad (18)$$

$$\Delta S°_s = (e^2/2r_+)\epsilon^{-2}(\partial\epsilon/\partial T) \quad (19)$$

where r_+ is the cation radius (see Table 1). Assuming that the molar volume of the *trans*-decalin$^{\bullet+}-$*tert*-butanol complex is equal to that of the constituents (264 cm^3 mol^{-1} for *trans*-decalin and 132.5 cm^3 mol^{-1} for *tert*-butanol)[28] we estimate $r_+ \approx 0.47$ nm for the hole (regarded as a radical cation) and $r_+ \approx 0.54$ nm for the complex, respectively. Therefore, the increases in $\Delta G°$ and $\Delta S°$ (as compared to gas-phase reaction (3)) from the ion solvation are around 10 kJ/mol and 5 J mol^{-1} K^{-1}, respectively; these values change little for alcohols other than *tert*-butanol. The largest correction comes from the solvation of the alcohol monomer. Unfortunately, almost no data on the thermodynamics of solvation is available for hydrocarbons. Wertz[31] found that, for all organic molecules in water, $\Delta S°_s \approx (S°_{liq} - S_{gas})(S°_{solute}/S_{gas}{}^{-1})$, where $S°_{liq}$ is the entropy of the liquid solvent, $S°_{solute}$ is the third law entropy of the gas-phase solute, and S_{gas} is the entropy of the solvent treated as an ideal gas compressed to the density of liquid. Because $S°_{liq}$ is not known for decalins, we used the data for cyclohexane[32] and obtained, using Wertz's equation,[31] $\Delta S°_{solv} \approx -0.195\,(S°_{solute} - 44.4$ J mol^{-1} K^{-1}), which gives estimates for the entropy of the solvation of methane, ethane, and cyclopropane in cyclohexane reasonably close to experimental values.[33] Using this formula and gas-phase entropies from ref 32, we estimated $\Delta S°_{solv}$ to be -45 J mol^{-1} K^{-1} for ethanol and $-(55-63)$ J

mol^{-1} K^{-1} for butanols. Thus, $\Delta S°$ for reaction (3) in the liquid should be 50−65 J mol^{-1} K^{-1} more positive than that in the gas phase.

5. Conclusion

In *cis*- and *trans*- decalins, proton-transfer reactions of solvent holes with aliphatic alcohols occur via the formation of metastable complexes with lifetimes to several tens of nanoseconds. The binding energies of these complexes are between 25 and 40 kJ/mol; proton transfer within the complex occurs over a 20−25 kJ/mol barrier. The complexation exhibits near-zero activation energy and occurs with rate constant of (1−1.2) × 10^{11} M^{-1} s^{-1} in *trans*-decalin and 3 × 10^{10} M^{-1} s^{-1} in *cis*-decalin. While the stability of the complex increases with the carbon number of the alcohol, the heat $-\Delta H°$ of the complexation decreases. This stability is mainly determined by the entropy $\Delta S°$ of complexation, which also correlates with $\Delta H°$. The entropy is small (−80 to 0 J mol^{-1} K^{-1}), and approaches zero for higher alcohols (in *trans*-decalin). In *cis*-decalin, $\Delta S°$ is ≈35 J mol^{-1} K^{-1} more positive, which explains greater stability of hole−solute complexes in this solvent. We argue that this thermochemistry is due to strong "solvation" of the hole.

Acknowledgment. Work performed under the auspices of the Office of Basic Energy Sciences, Division of Chemical Science, U.S. Department of Energy under Contract W-31-109-ENG-38.

Supporting Information Available: 1. Charge Recombination and the Reaction Kinetics. 2. Complications due to Association of Alcohol in Cycloalkanes. 3. Decay Kinetics and Arrhenius Plots for Rate Constants for Scavenging of Solvent Holes in *trans*- and *cis*-Decalin Liquids by Aliphatic Alcohols. This material is available free of charge via the Internet at http://pubs.acs.org.

References and Notes

(1) Sauer, M. C., Jr.; Shkrob, I. A.; Trifunac, A. D. Radiation Chemistry of Organic Liquids: Saturated Hydrocarbons. In *Radiation Chemistry: Present Status and Future Prospects*; Jonah, C. D., Rao, B. S. M., Eds.; Elsevier: Amsterdam, 2000.

(2) Trifunac, A. D.; Sauer, M. C., Jr.; Shkrob, I. A.; Werst, D. W. *Acta Chem. Scand.* **1997**, *51*, 158 and references therein.

(3) Sviridenko, F. B.; Stass, D. V.; Molin, Yu. N. *Chem. Phys. Lett.* **1998**, *297*, 343, and references therein.

(4) Tagawa, S.; Hayashi, N.; Yoshida, Y.; Washi, M.; Tabata, Y. *Radiat. Phys. Chem.* **1989**, *34*, 503.

(5) Warman, J. M. In *The Study of Fast Processes and Transient Species by Electron-Pulse Radiolysis*; Baxendale, J. H., Busi, F., Eds.; Reidel: The Netherlands, 1982; p 433.

(6) Beck, G.; Thomas, J. K. *J. Phys. Chem.* **1972**, *76*, 3856. Hummel, A.; Luthjens, L. H. *J. Chem. Phys.* **1973**, *59*, 654. Zador, E.; Warman, J. M.; Hummel, A. *Chem. Phys. Lett.* **1973**, *23*, 363; *75*, 914. *J. Chem. Phys.* **1975**, *62*, 3897; *J. Chem. Soc., Faraday Trans. 1* **1979**. de Haas, M. P.; Warman, J. M.; Infelta, P. P.; Hummel, A. *Chem. Phys. Lett.* **1975**, *31*, 382. *Chem. Phys. Lett.* **1976**, *43*, 321; *Can. J. Chem.* **1977**, *55*, 2249. Luthjens, L. H.; de Leng, H. C.; van den Ende, C. A. M.; Hummel, A. *Proc. 5th Symp. Radiat. Chem.* **1982**, 471. Hummel, A.; Luthjens, L. H. *J. Radioanal. Nucl. Chem., Art.* **1986**, *101*, 293. Sauer, M. C., Jr.; Schmidt, K. H. *Radiat. Phys. Chem.* **1988**, *32*, 281. Liu, A.; Sauer, M. C., Jr.; Trifunac, A. D. *J. Phys. Chem.* **1993**, *97*, 11265.

(7) Anisimov, O. A.; Warman, J. M.; de Haas, M. P.; de Leng, H. *Chem. Phys. Lett.* **1987**, *137*, 365.

(8) Warman, J. M.; de Leng, H. C.; de Haas, M. P.; Anisimov, O. A. *Radiat. Phys. Chem.* **1990**, *36*, 185.

(9) Shkrob, I. A.; Sauer, M. C., Jr.; Yan, J.; Trifunac, A. D. *J. Phys. Chem.* **1996**, *100*, 6876.

(10) Sauer, M. C., Jr.; Shkrob, I. A.; Yan, J.; Schmidt, K. H.; Trifunac, A. D. *J. Phys. Chem.* **1996**, *100*, 11325.

(11) Shkrob, I. A.; Liu, A. D.; Sauer, M. C., Jr.; Schmidt, K. H.; Trifunac, A. D. *J. Phys. Chem. B* **1998**, *102*, 3363.

(12) Shkrob, I. A.; Liu, A. D.; Sauer, M. C., Jr.; Schmidt, K. H.; Trifunac, A. D. *J. Phys. Chem. B* **1998**, *102*, 3371.

(13) Liu, A. D.; Shkrob, I. A.; Sauer, M. C., Jr.; Trifunac, A. D. *Radiat. Phys. Chem.* **1998**, *51*, 273.

(14) Shkrob, I. A.; Sauer, M. C., Jr.; Trifunac, A. D. *J. Phys. Chem.* **1999**, *103*, 4773.

(15) Gee, N.; Freeman, G. R. *J. Chem. Phys.* **1992**, *96*, 586.

(16) Lias, S. G.; Bartmess J. E.; Liedman, J. F.; Holmes J. L.; Levin, R. D.; Mallard, W. G. *Gas-Phase Ion and Neutral Thermochemistry*; American Chemical Society/American Institute of Physics: Washington, DC/New York, 1988. Issued as *J. Phys. Chem. Ref. Data* **1988**, *17*, Supplement 1.

(17) Sieck, L. W.; Searles, S. K. *J. Chem. Phys.* **1970**, *53*, 2601; DeCorpo, J. J.; McDowell, M. V.; Saalfield, F. E. *J. Phys. Chem.* **1972**, *76*, 1517.

(18) Johnston D. B.; Lipsky, S. *Radiat. Phys. Chem.* **1991**, *38*, 51.

(19) Johnston D. B.; Wang, Y.-M.; Lipsky, S. *Radiat. Phys. Chem.* **1991**, *38*, 583.

(20) Shkrob, I. A.; Sauer, M. C., Jr.; Trifunac, A. D. *J. Phys. Chem.* **2000**, *104*, 3760.

(21) Badger, B.; Brocklehurst, B. *Trans. Faraday Soc.* **1969**, *65*, 2582; **1970**, *66*, 2939.

(22) Shkrob, I. A.; Sauer, M. C., Jr.; Liu, A. D.; Crowell, R. A.; Trifunac, A. D. *J. Phys. Chem. A* **1998**, *102*, 4976.

(23) From our AM1 calculations and data for analogous radicals reported in a review article by McMillen, D. F.; Golden D. M. *Annu. Rev. Phys. Chem.* **1982**, *33*, 493.

(24) Walder, R.; Franklin, J. L. *Int. J. Mass. Spectrom. Ion Phys.* **1980**, *36*, 85.

(25) Knochenmuss, R.; Leutwyler, S. *J. Chem. Phys.* **1989**, *91*, 1268.

(26) Stokes, R. H. *J. Chem. Soc., Faraday Trans. 1* **1977**, *73*, 1140.

(27) Smith, F. *Austral. J. Chem.* **1976**, *23*, 43.

(28) Grigoriev, I. S.; Meilikhov, E. Z. *Handbook of Physical Quantities*; CRC Press: Boca Raton, FL, 1997; p 399.

(29) Hanna, M. W.; Lippert, J. L. In *Molecular Complexes*; Foster, R., Ed.; Crane, Russak & Co.: New York, 1973; Vol. 1, p 1.

(30) Pimentel, G. C.; McClellan, A. L. *The Hydrogen Bond*; Freeman: London, 1960; Chapter 7.

(31) Wertz, D. H. *J. Am. Chem. Soc.* **1980**, *102*, 5316.

(32) Frenkel, M.; Marsh, K. N.; Wilhoit, R. C.; Kabo, G. J.; Roganov, G. N. *Thermodynamics of Organic Compounds in the Gas State*; TRC Data Series; Thermodynamics Research Center: College Station, TX, 1994; *Selected Values of Properties of Hydrocarbons*; American Petroleum Institute Research Project 44; U.S. Department of Commerce, National Bureau of Standards: Washington, DC; Tables 23-2-(3.100)-p, p 1.

(33) Dymond, J. H. *J. Phys. Chem.* **1967**, *71*, 1829.

(34) *Handbook of Chemistry and Physics*; Weast, R. C., Astle, M. J., Eds.; CRC Press: Boca Raton, FL, 1981.

(35) Fischer, J.; Weiss, A. *Ber. Bunsen-Ges. Phys. Chem.* **1986**, *90*, 896. Gonçalves, F. A.; Hamano, K.; Sengers, J. V. *Int. J. Thermophys.* **1989**, *10*, 845.